www.nature.com/modpathol

ARTICLE

Potential pathogenetic link between angiomyofibroblastoma and superficial myofibroblastoma in the female lower genital tract based on a novel *MTG1-CYP2E1* fusion

Ryosuke Tajiri[1,2], Eisuke Shiba[1], Ryuji Iwamura[1], Chisachi Kubo[1], Aya Nawata[1], Hiroshi Harada[2], Kiyoshi Yoshino[2] and Masanori Hisaoka[1]✉

Angiomyofibroblastoma and superficial myofibroblastoma are distinctive benign mesenchymal tumors occurring in the female lower genital tract. Despite their significant overlapping clinicopathologic features, including the presence of bland-looking spindle or oval cells with myofibroblastic or myoid differentiation, the tumors have been regarded as separate entities. Although subepithelial, hormone-sensitive mesenchymal cells of the female lower genital tract are considered as their potential common progenitor cells, their potential kinship or pathogenetic similarities remain elusive. Based on the identification of a novel RNA sequencing-based MTG1-CYP2E1 fusion transcript in an angiomyofibroblastoma index case, we investigated an additional ten samples of the tumor and its site-specific histological mimics, including eight superficial myofibroblastomas, four deep angiomyxomas, four cellular angiofibromas, three fibroepithelial stromal polyps, and eight non-site-specific mesenchymal tumors occurring in the female lower genital tract. Using reverse transcription-polymerase chain reaction, we showed that the MTG1-CYP2E1 fusion transcripts were consistently detectable in angiomyofibroblastomas (5/5, 100%) and often in superficial myofibroblastomas (3/5, 60%) but were not detected in the other examined site-specific or non-site-specific mesenchymal tumors. Our immunohistochemical experiments showed that CYP2E1, an isoenzyme belonging to the cytochrome P450 superfamily, exhibited increased positivity in tumors with *MTG1-CYP2E1* than was observed in fusion-negative tumors (RR = 6.56, $p = 0.001$). The results of our study provide further evidence supporting the assertion that angiomyofibroblastoma and superficial myofibroblastoma represent phenotypic variants of site-specific mesenchymal tumors and share a common oncogenic mechanism.

Modern Pathology (2021) 34:2222–2228; https://doi.org/10.1038/s41379-021-00886-8

INTRODUCTION

The female lower genital tract, a specialized portion of the female reproductive system, is characterized by squamous epithelial lining and an underlying band of loose fibrovascular stroma extending from the uterine cervix to the vulva, potentially accounting for its physical plasticity[1]. A variety of mesenchymal tumors may develop in the female lower genital tract, which characteristically include angiomyofibroblastoma, superficial (cervicovaginal) myofibroblastoma, deep (or aggressive) angiomyxoma, and cellular angiofibroma[2].

Angiomyofibroblastoma is a rare but well-described benign mesenchymal tumor that occurs almost exclusively as a vulvovaginal lesion. It is composed of a proliferation of plump oval or epithelioid cells arranged characteristically in a perivascular pattern, and with consistent expression of the receptor proteins for estrogen (ER) and progesterone (PgR). Furthermore, the tumor often demonstrates a unique myoid differentiation, typically characterized by a desmin-positive and actin-negative immunophenotype[2–5]. Hormone-responsive stromal cells, located in the subepithelial myxoid zone in the lower female genital tract or perivascular stem cells, have been implicated as a potential progenitor of angiomyofibroblastoma[3,6].

Superficial (cervicovaginal) myofibroblastoma is a relatively recently recognized mesenchymal neoplasm arising from the superficial portion of the lower genital tract in females of a much wider age range than those presenting with angiomyofibroblastoma[7,8]. Despite a few variegated histological patterns, the tumor cells are usually spindle or oval, displaying a wavy appearance, embedded in a finely or thick collagenous stroma, and are immunohistochemically positive for vimentin, desmin, ER, and PgR, as observed in angiomyofibroblastoma. It has also been assumed that the tumor is derived from the subepithelial band-like stromal zone as in angiomyofibroblastoma, despite certain unique clinicopathological features, including a somewhat distinct localization and cytomorphology, that can be considered to justify the classification of these tumors as separate entities.

The pathogenic mechanisms underlying the development of these tumors, however, remain largely unclear. No molecular genetic alterations, including those in *RB1/FOXO1* and *HMGA2*, have been described in cases of angiomyofibroblastoma, with

[1]Department of Pathology and Oncology, School of Medicine, University of Occupational and Environmental Health, Kitakyushu, Japan. [2]Department of Obstetrics and Gynecology, School of Medicine, University of Occupational and Environmental Health, Kitakyushu, Japan. ✉email: hisaoka@med.uoeh-u.ac.jp

Received: 13 May 2021 Revised: 15 July 2021 Accepted: 15 July 2021
Published online: 12 August 2021

only a single case expressing HMGA2 transcripts[5,9,10], whereas such genomic changes are detectable in its potential histological mimics, including mammary type myofibroblastoma, cellular angiofibroma, and deep angiomyxoma[11–13]. This finding may be in line with the notion that angiomyofibroblastoma is a distinct entity from such other site-specific mesenchymal tumors, despite their overlapping clinicopathological features that often pose diagnostic challenges. We hypothesized that a hitherto unrecognized molecular alteration might exist and contribute to the development of such rare site-specific mesenchymal tumors[14–16].

In this study, we examined a case of angiomyofibroblastoma using next-generation RNA sequencing and extended the study to focus on a potential molecular genetic alteration that was identified, examining a series of cases of the tumor and its histological mimics to further our understanding of such site-specific mesenchymal tumors in the lower female genital tract.

MATERIALS AND METHODS

Cases

Data on the subjects and their clinical information were retrieved from the files of the Department of Pathology and Oncology, School of Medicine, University of Occupational and Environmental Health (UOEH), Japan, and from personal consultation files of one of the authors (M.H.). After a critical review of the archival materials of each case, the study cohort was established and comprised thirty cases of site-specific mesenchymal tumors/lesions, including eleven angiomyofibroblastomas, eight superficial myofibroblastomas, four deep angiomyxomas, four cellular angiofibromas, and three fibroepithelial stromal polyps. Eight cases of selected non-site-specific tumors arising in the female lower genital tract (i.e., four leiomyomas, two mammary type myofibroblastomas, one solitary fibrous tumor, and one spindle cell lipoma) were also included in the study. No snap-frozen tumor tissue was available for investigation in this cohort. The study was approved by the Institutional Review Board of UOEH. Further clinical information and the obtained data for each subject are depicted in Supplementary Table 1.

RNA sequencing

We initially selected a few cases of angiomyofibroblastoma with sufficient formalin-fixed, paraffin-embedded (FFPE) tumor tissues, from which total RNA extraction was performed using the TRIzol reagent (Thermo Fischer Scientific, Tokyo, Japan). One microgram of the purified RNA and an RNeasy FFPE kit (Qiagen, Hilden, Germany) were used for whole-transcriptome RNA sequencing (Cell Innovator, Fukuoka, Japan). After performing a rigorous quality check using the 2100 Bioanalyzer (Agilent, Santa Clara, CA) and a FastQC quality control program (version 0.11.9, Macrogen, Seoul, South Korea), one of the submitted samples was considered amenable for subsequent sequence analysis using the Illumina MiSeq platform (Illumina, San Diego, CA). Reads were mapped to the human reference genome (hg38) using the HISAT2 program (http://daehwankimilab.github.io/hisat2/) and analyzed using the STAR-Fusion pipeline (version 1.9.1)[17].

Reverse transcription-polymerase chain reaction (RT-PCR)

Briefly, RNA samples extracted from the FFPE tissues were reverse-transcribed into cDNA and used as a template for conducting PCR for the *MTG1-CYP2E1* fusion. Specific primers designed in-house were as follows: MTG1-forward (5′-ACCATGGCTGACTACCTGCT) and CYP2E1-reverse (5′-GCCAGAAGGAAAATTCAACATAC) primers. PCR was conducted under the following conditions: 95 °C for 9 min, followed by 40 cycles of 95 °C for 10 s, 61 °C for 10 s, and 72 °C for 10 s, followed by a final extension at 72 °C for 10 min. The integrity of RNA was assessed by performing PCR for the representative housekeeping genes such as phosphoglycerate kinase gene (PGK, size = 247 bp) and porphobilinogen deaminase gene (PBGD, size = 127 bp). Sequences of the amplified PCR products were determined by conducting the Sanger method using the 3500xL genetic analyzer (Thermo Fischer Scientific).

Immunohistochemistry

Expression of MTG1 and CYP2E1 in tumor cells was assessed immunohistochemically using primary mouse polyclonal anti-MTG1 and anti-CYP2E1 antibodies (Supplementary Table 2). Staining results were initially evaluated and scored on a scale of 1+ to 3+ as follows: 1+, weak staining in 1–25% of the tumor cells; 2+, weak to moderate staining in 25–50% of the tumor cells, and 3+, strong staining in more than 50% of the tumor cells[18]. Tumors with expression levels labeled as 2+ or 3+ were considered to exhibit unequivocal expression and then as 'positive' cases. Appropriate positive controls were included in the study (i.e., tissues of the lymph node for MTG1 and the liver for CYP2E1)[19,20]. For negative controls, the primary antibody was substituted with phosphate-buffered saline (PBS). A potential correlation between the results obtained by RT-PCR and those obtained by immunohistochemistry was statistically examined using the Fisher's exact test.

RESULTS

MTG1-CYP2E1 fusion in angiomyofibroblastoma

In the index case (#1) of angiomyofibroblastoma with well-preserved RNA, reads encompassing a sequence of exon 9 (NM_138384.4) of the *MTG1* gene fused to the 5′ regulatory region (NG_055447.1) of the *CYP2E1* gene were detected by using the RNA sequencing platform (Fig. 1A, B). Both the *MTG1* and *CYP2E1* genes localize at chromosome 10q26.3, within 125 kb of each other, and in which the gene rearrangement could not be demonstrated easily in tumor cell nuclei in FFPE tissues using a conventional fluorescence in situ hybridization technique (Fig. 1C). The fusion sequence of MTG1-CYP2E1 was further confirmed by conducting RT-PCR and Sanger sequencing in the same case (Fig. 1D). Additional angiomyofibroblastoma cases were examined for the MTG1-CYP2E1 fusion by RT-PCR, and all cases with evaluable mRNA were termed fusion-positive (Table 1, Supplementary Table 1).

MTG1-CYP2E1 in other site-specific mesenchymal tumors and histological mimics

RT-PCR for the MTG1-CYP2E1 fusion was performed in a variety of site-specific mesenchymal tumors other than angiomyofibroblastoma. Fusion was detected in three of the five superficial myofibroblastomas examined, whereas the other site-specific tumors/lesions or histological mimics arising in the female lower genital tract were negative for the fusion, irrespective of the amplified mRNA sequences of the housekeeping genes (i.e., PBGD and/or PGK) (Fig. 1D, Table 1, Supplementary Table 1).

Clinicopathological features

The study cohort included 11 patients with angiomyofibroblastoma in the vulva, ranging in age from 23 to 61 years (median: 42 years, mean: 41 years), 8 patients with superficial myofibroblastoma in the vagina (5 cases), vulva (2 cases), or uterine cervix (1 case) with ages ranging from 26 to 74 years (median: 46 years, mean: 50 years), and 19 patients with 11 other site-specific and 8 non-site-specific mesenchymal tumors of various histological types in the lower female genital tract except for some cases with deep angiomyxoma (2 cases), cellular angiofibroma (1 case), and mammary type myofibroblastoma (1 case), which affected the male inguino-genital region (Supplementary Table 1).

All cases of angiomyofibroblastoma focally showed at least its classical morphologic features: well-demarcated subcutaneous nodular lesions with sizes ranging from 1 to 14 cm in diameter, composed of an alternating cellular and a less cellular proliferation of short spindle, oval, or epithelioid cells arranged in small groups or cords with a tendency to aggregate around dilated small blood vessels and embedded in a well-vascularized fibromyxoid or edematous stroma (Fig. 2A–C). A variable amount of intratumoral adipocytic component, ranging from ~10 to 50% of the tumor area, was present in four cases (Fig. 2B). Unusual perivascular fibrosclerosis was seen in one angiomyofibroblastoma. All but two cases were immunohistochemically positive for desmin to various extents, although other smooth muscle markers (i.e., smooth muscle actin, calponin, and h-caldesmon) were negative (Supplementary Table 1).

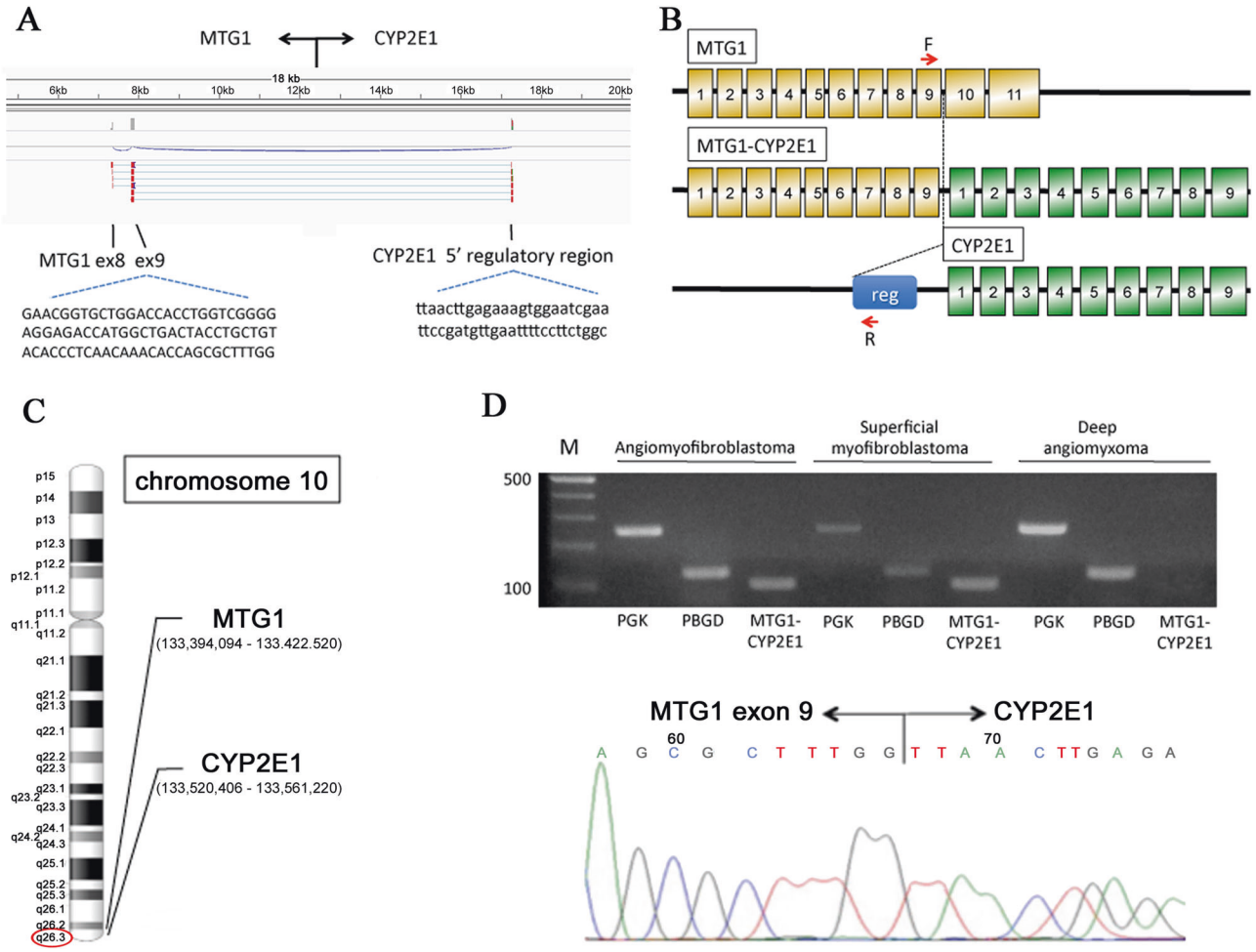

Fig. 1 Schematic representations and site-specific molecular detections of the MTG1-CYP2E1 fusion in mesenchymal tumors. A Reads representing fusion transcripts between exon 9 of *MTG1* and the 5′ regulatory region of *CYP2E1* identified via RNA sequencing in a case of angiomyofibroblastoma; (**B**) in the *MTG1-CYP2E1* fusion, exons 10 and 11 located in the 3′-terminus of *MTG1* were replaced by an entire CYP2E1 RNA sequence. Red arrows indicate specific primers used for the following RT-PCR; (**C**) *MTG1* and *CYP2E1* localization at a distal portion of the long arm of chromosome 10. The genomic positions of the genes are described within parentheses according to the database of GRCh38.p13; (**D**) RT-PCR conducted for MTG1-CYP2E1 showing visible 100-bp bands for angiomyofibroblastoma and superficial myofibroblastoma (upper panel) samples. Sanger sequencing of the PCR product, demonstrating a fusion between *MTG1* exon 9 and the 5′ regulatory region of *CYP2E1*.

Table 1. Expression of MTG1 and CYP2E1 or fusion transcript in mesenchymal tumors.

Tumor	IHC[a]		RT-PCR[b]
	MTG1 positive (%)	CYP2E1 positive (%)	MTG1-CYP2E1 fusion positive (%)
Site-specific			
Angiomyofibroblastoma	7/9 (78)	10/11 (91)	5/5 (100)
Superficial myofibroblastoma	4/8 (50)	7/8 (88)	3/5 (60)
Deep angiomyxoma	3/4 (75)	0/4 (0)	0/1 (0)
Cellular angiofibroma	0/4 (0)	0/4 (0)	0/2 (0)
Fibroepithelial stromal polyp	0/3 (0)	0/3 (0)	0/2 (0)
Non-site-specific			
Leiomyoma	0/4 (0)	0/4 (0)	0/4 (0)
Solitary fibrous tumor	0/1 (0)	0/1 (0)	0/1 (0)
Myofibroblastoma (mammary type)	0/2 (0)	0/2 (0)	0/2 (0)
Spindle cell lipoma	0/1 (0)	0/1 (0)	0/1 (0)

[a]Number of cases depicted.
[b]Positive cases/all cases examined.

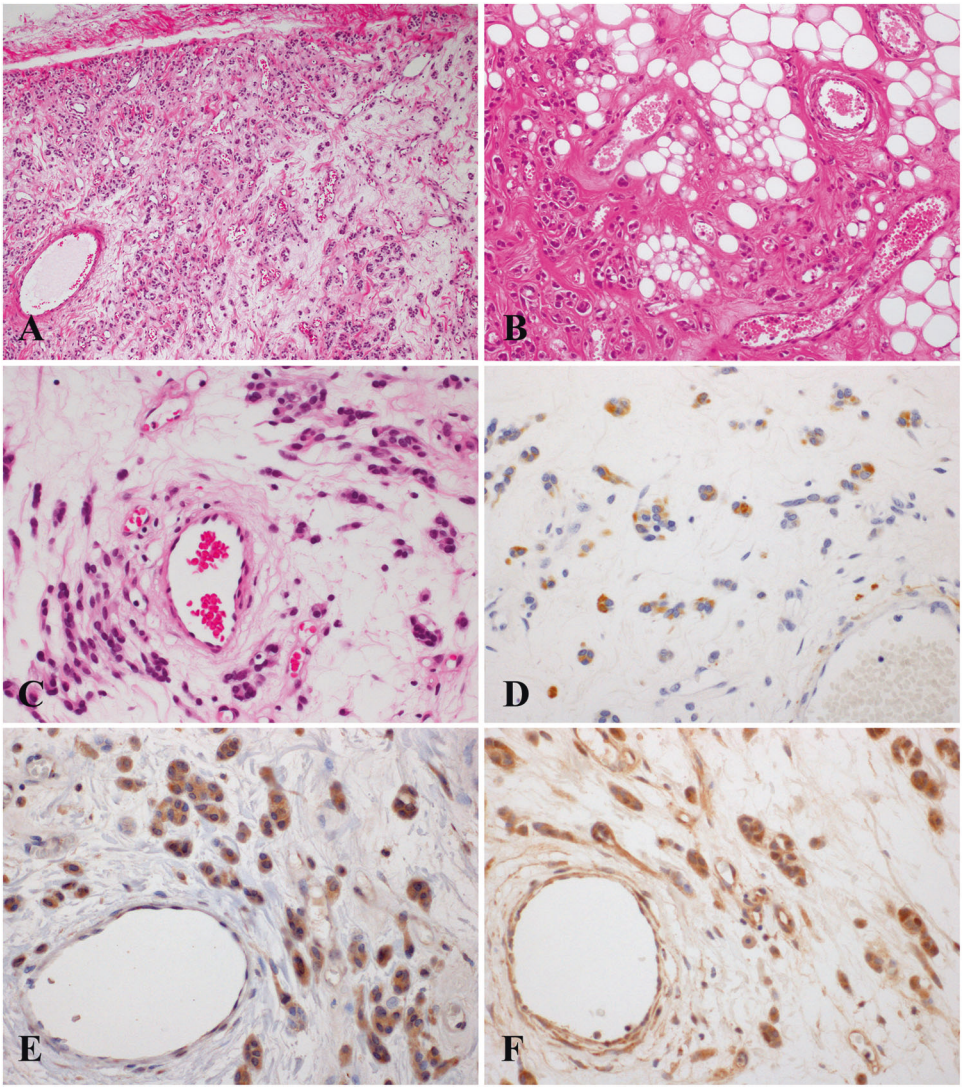

Fig. 2 Angiomyofibroblastoma. A A well-demarcated lesion made up of alternating hypocellular edematous and cellular areas with a well-vascularized stroma (H&E). **B** An adipocytic component within the tumor (H&E). **C** Perivascular arrangement of plump oval or epithelioid cells in a loose edematous stroma (H&E). Immunohistochemical staining results highlighting (**D**) desmin expression in tumor cells, (**E**) intense granular CYP2E1 expression (scored as 2+) in tumor cells, and (**F**) MTG1 expression (scored as 2+) in tumor cells and a few bystander cells such as vascular endothelial cells.

The superficial myofibroblastomas assessed in the study were well-demarcated superficial or subepithelial nodular lesions predominantly composed of bland spindle, oval, or stellate-shaped cells arranged in multiple histological patterns, including an almost diffuse haphazard, lacelike, or sievelike pattern with a fibrocollagenous, myxoid, or edematous stroma and at least focal immunohistochemical expression of smooth muscle markers (Fig. 3A–C). No distinct clinicopathological feature was identified among the cases with or without immunohistochemical expression of CYP2E1 described below or MTG1-CYP2E1 fusion.

The other site-specific or non-site-specific mesenchymal tumors or lesions had almost typical or conventional clinicopathological features together with the corresponding supportive immunohistochemical findings, such as nuclear HMGA2 expression in deep fibromyxoma and loss of RB1 expression in cellular angiofibroma in selected cases (Fig. 4A–C).

Immunohistochemical staining of MTG1 and CYP2E1

The immunohistochemical staining of MTG1 and CYP2E1 showed that they were expressed in varying intensities in a variety of the examined site-specific or non-site-specific mesenchymal tumors or lesions (Supplementary Table 1). In contrast to the relatively non-specific and often less intense staining intensity observed for MTG1, the CYP2E1 expression was almost exclusively confined to angiomyofibroblastoma and superficial myofibroblastoma with or without detectable MTG1-CYP2E1 fusion, in which an unequivocal or intense intracytoplasmic and often granular staining was observed (Figs. 2–4, Table 1). Additionally, the immunohistochemical results for CYP2E1 showed a statistical correlation with those obtained by RT-PCR (R.R. = 6.56, $p = 0.001$ using the Fisher's exact test).

DISCUSSION

In this study, we described a gene fusion occurring between *MTG1* and *CYP2E1* in vulval angiomyofibroblastoma and superficial myofibroblastoma. In the RNA sequencing analysis, the gene fusion was suggested between a relatively distal portion of *MTG1* and a 5′-regulatory region of *CYP2E1*, leading to a juxtaposition of the entire coding region of CYP2E1 mRNA with a truncated MTG1

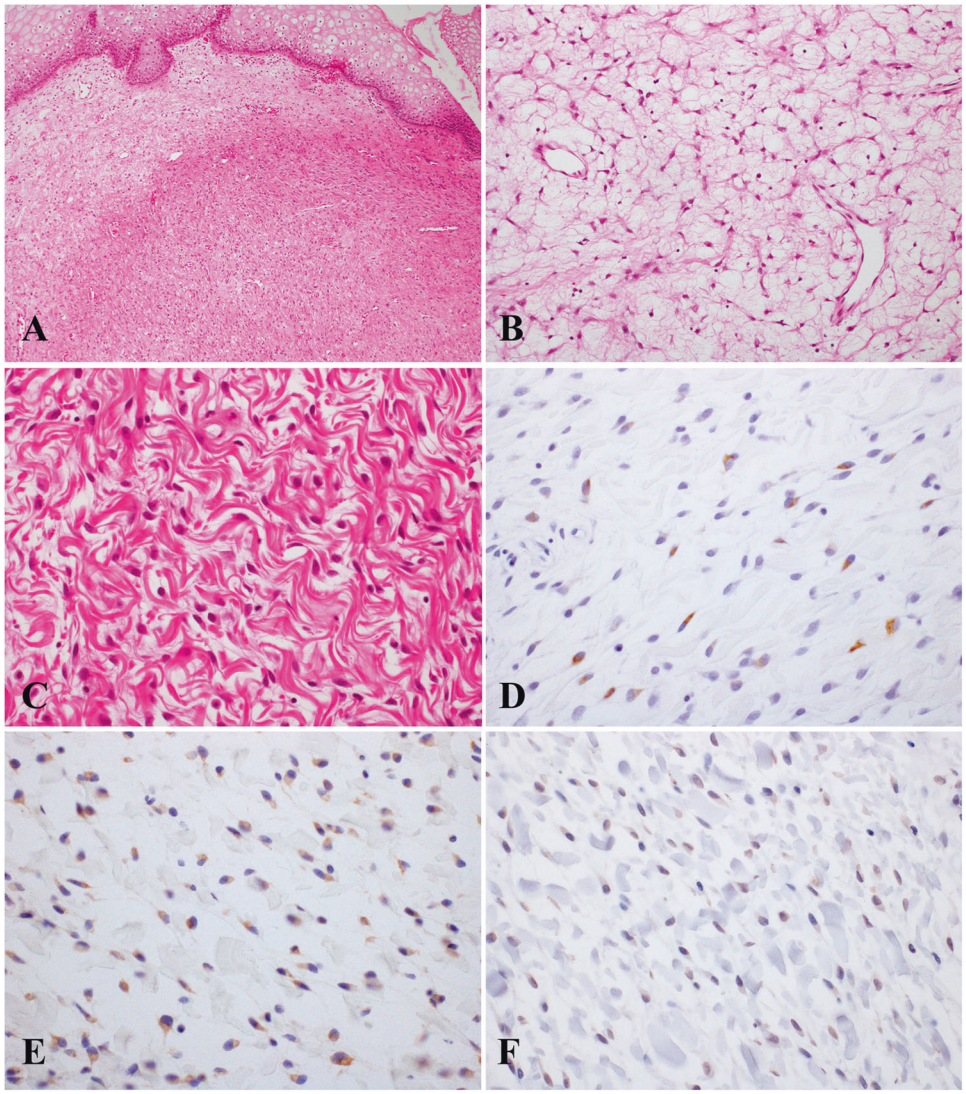

Fig. 3 Superficial myofibroblastoma. A A well-demarcated superficial lesion with a subepithelial loose edematous stroma (H&E). **B** A lacelike arrangement of spindle or stellate-shaped cells embedded in an abundant myxoid background (H&E). **C** Short spindle cells embedded in finely fibrillar or wavy collagen (H&E). Immunohistochemical staining results highlighting (**D**) desmin-positivity in a few tumor cells, (**E**) moderate CYP2E1 expression (scored as 2+) in tumor cells, and (**F**) focal and mild MTG1 expression (scored as 1+) in tumor cells.

mRNA. The fusion is assumed to result in aberrant activation or expression of *CYP2E1* under the control of the *MTG1* promoter as MTG1 is almost ubiquitously expressed in contrast to CYP2E1, which is essentially confined to hepatocytes according to a comprehensive database (the Human Protein Atlas) for spatial protein distribution in human tissues and cells[17].

Both *MTG1* and *CYP2E1* are localized to chromosome 10q26.3, and *MTG1* is mapped in the vicinity of the 5′ end of *CYP2E1* within a distance of approximately 125 kb, which also encompasses several genes or pseudogenes such as *OR6L2P*, *SCART1*, and *OR7M1P*. An interstitial microdeletion in chromosome 10q26.3 is considered a potential genomic alteration that may result in the *MTG1-CYP2E1* fusion, although high-resolution molecular genetic analyses, such as array comparative genomic hybridization, are needed to demonstrate such a cryptic genomic imbalance.

MTG1 encodes a protein that functions as a member of the GTPase family located in the mitochondrial inner membrane and is involved in mitochondrial ribosome assembly, ensuring mitochondrial translation[18]. Genomic alterations of *MTG1* have been poorly investigated, and to the best of our knowledge, only a gene fusion of *MTG1* and *ZFN511*, the latter of which also maps to chromosome 10q26.3, has been described in breast carcinoma[19]. CYP2E1 is an isoenzyme belonging to the cytochrome P450 superfamily, which is mainly expressed in the liver and plays an important role in the metabolism of drugs or environmental toxicants, including nitrosamines, benzene, and ethanol[20]. Additionally, the oncogenic role of highly expressed CYP2E1 has been described in gastric, breast, and liver cancers[21–23]. Notably, female sex steroid hormones can enhance CYP2E1 expression in mouse livers[24]. Thus, hormone-sensitive stromal cells in the female genital tract may also be susceptible to tumorigenesis mediated by aberrantly expressed CYP2E1. Although genetic polymorphism in *CYP2E1*, probably related to susceptibility to hepatic cirrhosis or cancers, has been identified in the population[25], no gene fusion involving *CYP2E1* has been described in the literature.

The aberrant expression of CYP2E1, presumably induced by the *MTG1-CYP2E1* fusion, was validated by the results of the immunohistochemical analysis conducted herein using an anti-CYP2E1 antibody, which demonstrated an intense and often granular cytoplasmic staining in the mesenchymal tumors harboring the *MTG1-CYP2E1* fusion but not in those without detectable *MTG1-CYP2E1*. Focal or faint CYP2E1 expression

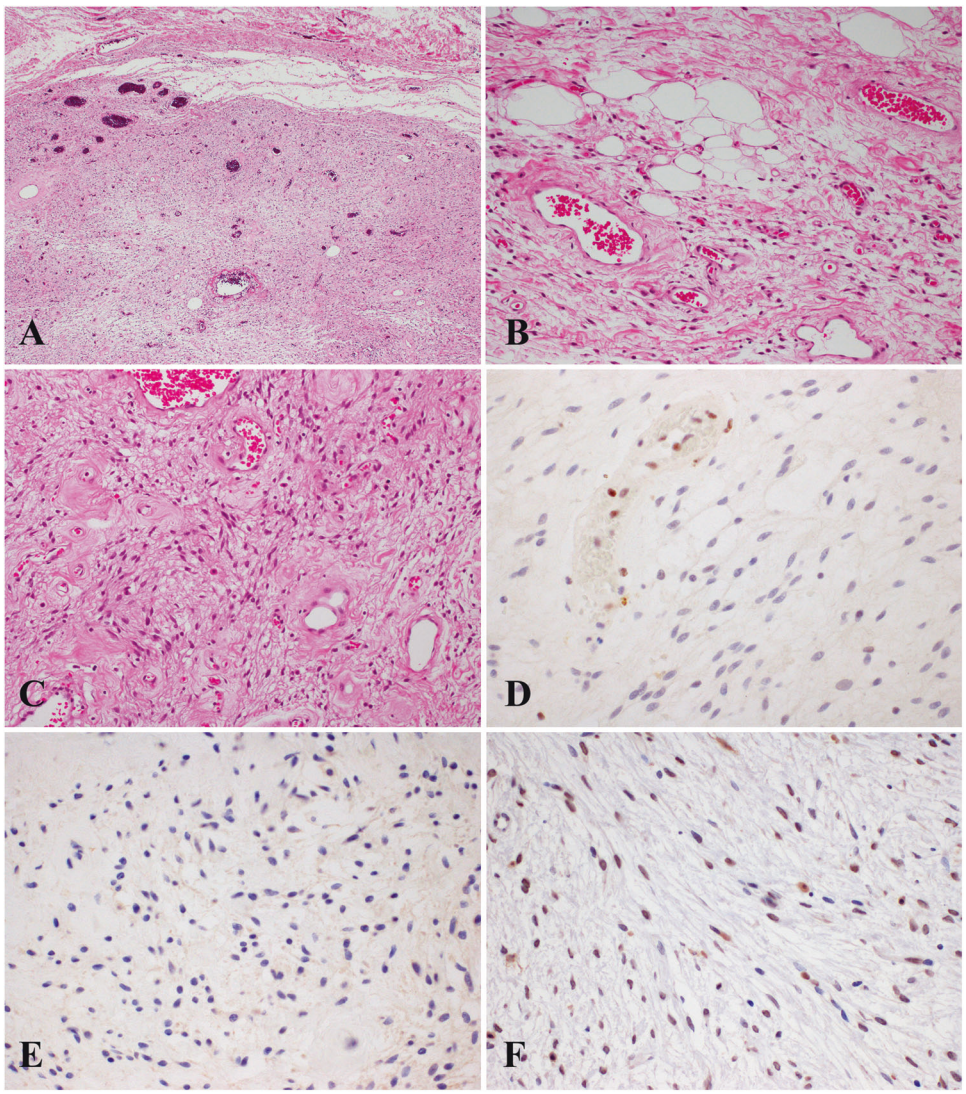

Fig. 4 Cellular angiofibroma. A A well-demarcated and well-vascularized lesion (H&E). **B** A minor adipocytic component mainly in the peripheral area (H&E). **C** Bland-appearing spindle cells with an abundant fibrous stroma and dilated blood vessels exhibiting sclerotic walls (H&E). Immunohistochemical staining results highlighting (**D**) the loss of nuclear RB1 expression (nuclear positivity could be noted in the endothelial cells), (**E**) the lack of CYP2E1 expression in the tumor cells, and (**F**) mild MTG1 expression (scored as 1+) in the spindle cells and some inflammatory cells.

observed in a few fusion-undetectable cases may reflect a physiological response to sex steroid hormones in such hormone-responsive mesenchymal cells.

Another salient feature of our study is that the *MTG1-CYP2E1* and aberrant CYP2E1 expression were detected only in angiomyofibroblastoma and superficial myofibroblastoma, suggesting a close association between these tumor entities. Based on their overlapping clinicopathological features, including myofibroblastic or myoid differentiation, both tumors may belong to a single tumor spectrum derived from hormone-responsive mesenchymal cells in the female genital tract. However, the potential diagnostic utility of CYP2E1 as a surrogate marker for angiomyofibroblastoma and superficial myofibroblastoma warrants further investigation using more cases of a variety of tumor types.

In summary, the identification of the gene fusion *MYG1-CYP2E*1 in an index case of angiomyofibroblastoma by RNA sequencing led us to expand our investigation of this novel genetic alteration to include a variety of site-specific mesenchymal tumors in the female lower genital tract. The fusion was found to be confined to angiomyofibroblastoma and superficial myofibroblastoma, and enhanced immunohistochemical expression of CYP2E1 probably resulted from gene alterations in the tumors. This finding suggests that angiomyofibroblastoma and superficial myofibroblastoma belong to a common spectrum of mesenchymal tumors in such an anatomical location. In addition to a potential nosologic refinement, our study has the potential to accelerate analyses on the molecular mechanisms involved in site-specific tumor biology in the female genital tract. Because of the rarity of the tumors examined, the study has some limitations such as a small sample size, limited tumor types, and data obtained from archival materials (i.e., FFPE tissues).

REFERENCES

1. Elliott, G. B. & Elliott, J. D. Superficial stromal reactions of lower genital tract. *Arch Pathol.* **95**, 100–101 (1973).
2. McCluggage, W. G. A review and update of morphologically bland vulvovaginal mesenchymal lesions. *Int. J. Gynecol. Pathol.* **24**, 26–38 (2005).
3. Fletcher, C. D., Tsang, W. Y., Fisher, C., Lee, K. C. & Chan, J. K. Angiomyofibroblastoma of the vulva. A benign neoplasm distinct from aggressive angiomyxoma. *Am. J. Surg. Pathol.* **16**, 373–382 (1992).

4. Hisaoka, M., Kouho, H., Aoki, T., Daimaru, Y. & Hashimoto, H. Angiomyofibroblastoma of the vulva: a clinicopathologic study of seven cases. *Pathol. Int.* **45**, 487–492 (1995).
5. Magro, G., Righi, A., Caltabiano, R., Casorzo, L. & Michal, M. Vulvovaginal angiomyofibroblastomas: morphologic, immunohistochemical, and fluorescence in situ hybridization analysis for deletion of 13q14 region. *Hum. Pathol.* **45**, 1647–1655 (2014).
6. Laskin, W. B., Fetsch, J. F. & Tavassoli, F. A. Angiomyofibroblastoma of the female genital tract: analysis of 17 cases including a lipomatous variant. *Hum. Pathol.* **28**, 1046–1055 (1997).
7. Laskin, W. B., Fetsch, J. F. & Tavassoli, F. A. Superficial cervicovaginal myofibroblastoma: fourteen cases of a distinctive mesenchymal tumor arising from the specialized subepithelial stroma of the lower female genital tract. *Hum. Pathol.* **32**, 715–725 (2001).
8. Ganesan, R., McCluggage, W. G., Hirschowitz, L. & Rollason, T. P. Superficial myofibroblastoma of the lower female genital tract: report of a series including tumours with a vulval location. *Histopathology* **46**, 137–143 (2005).
9. Medeiros, F. et al. Frequency and characterization of HMGA2 and HMGA1 rearrangements in mesenchymal tumors of the lower genital tract. *Genes Chromosom. Cancer* **46**, 981–990 (2007).
10. Horiguchi, H. et al. Angiomyofibroblastoma of the vulva: report of a case with immunohistochemical and molecular analysis. *Int. J. Gynecol. Pathol.* **22**, 277–284 (2003).
11. Kazmierczak, B. et al. Cloning and molecular characterization of part of a new gene fused to HMGIC in mesenchymal tumors. *Am. J. Pathol.* **152**, 431–435 (1998).
12. Flucke, U., van Krieken, J. H. & Mentzel, T. Cellular angiofibroma: analysis of 25 cases emphasizing its relationship to spindle cell lipoma and mammary-type myofibroblastoma. *Mod. Pathol.* **24**, 82–89 (2011).
13. Magro, G. et al. Mammary and vaginal myofibroblastomas are genetically related lesions: fluorescence in situ hybridization analysis shows deletion of 13q14 region. *Hum. Pathol.* **43**, 1887–1893 (2012).
14. Henderson, S. R. et al. A molecular map of mesenchymal tumors. *Genome Biol.* **6**, R76 (2005).
15. McCluggage, W. G. Vulvovaginal mesenchymal lesions: a review and update. *Diagn. Histopathol.* **24**, 1–17 (2018).
16. Schneider, G., Schimidt-Supprian, M., Rad, R. & Saur, D. Tissue-specific tumorigenesis: context matters. *Nat. Rev. Cancer* **17**, 239–253 (2017).
17. Thul, P. J. & Lindskog, C. The human protein atlas: a spatial map of the human proteome. *Protein Sci.* **27**, 233–244 (2018).
18. Barrientos, A. et al. MTG1 codes for a conserved protein required for mitochondrial translation. *Mol. Biol. Cell* **14**, 2292–2302 (2003).
19. Yoshihara, K. et al. The landscape and therapeutic relevance of cancer-associated transcript fusions. *Oncogene* **34**, 4845–4854 (2015).
20. Gonzalez, F. J. Role of cytochromes P450 in chemical toxicity and oxidative stress: studies with CYP2E1. *Mutat. Res.* **569**, 101–110 (2005).
21. Leung, T. et al. Cytochrome P450 2E1 (CYP2E1) regulates the response to oxidative stress and migration of breast cancer. *Breast Cancer Res.* **15**, R107 (2013).
22. Gao, J. et al. Changes in cytochrome P450s-mediated drug clearance in patients with hepatocellular carcinoma in vitro and in vivo: a bottom-up approach. *Oncotarget* **7**, 28612–28623 (2016).
23. Wang, R. Y. et al. CYP2E1 changes the biological function of gastric cancer cells via the PI3K/Akt/mTOR signaling pathway. *Mol. Med. Rep.* **21**, 842–850 (2020).
24. Konstandi, M., Cheng, J. & Gonzalez, F. J. Sex steroid hormones regulate constitutive expression of *Cyp2e1* in female mouse liver. *Am. J. Physiol. Endocrinol. Metab.* **304**, E1118–E1128 (2013).
25. Neafsey, P. et al. Genetic polymorphism in CYP2E1: population distribution of CYP2E1 activity. *J. Toxicol. Environ. Health B Crit. Rev.* **12**, 362–388 (2009).

ACKNOWLEDGEMENTS

The authors are grateful to Dr. Noriyuki Iwama from the Department of Diagnostic Pathology, Tohoku Rosai Hospital, Japan, and Dr. Kosuke Makihara from the Department of Surgical Pathology, Kyushu Rosai Hospital, Japan, for providing tissue materials for this study cohort. We also thank Dr. Atsuji Matsuyama from the Division of Pathology and Laboratory Medicine, Fukuoka Wajiro Hospital, Japan, for his valuable comments on RNA sequencing and data analysis.

AUTHOR CONTRIBUTIONS

R.T. and M.H. conceived and designed the study, performed the data analysis and interpretation, and prepared the manuscript; E.S., R.I., C.K., and A.N. performed the acquisition, analysis, and interpretation of the data; and H.H. and K.Y. acquired clinical information. All authors read and approved the final version of the manuscript before submission.

COMPETING INTERESTS

The authors declare no competing interests.

ETHICS APPROVAL

IRB approval status: this study was reviewed and approved by the Ethics Committee of Medical Research, University of Occupational and Environmental Health, Japan (Ref. No. 19-065)

ADDITIONAL INFORMATION

Supplementary information The online version contains supplementary material available at https://doi.org/10.1038/s41379-021-00886-8.

Correspondence and requests for materials should be addressed to M.H.

Reprints and permission information is available at http://www.nature.com/reprints

Publisher's note Springer Nature remains neutral with regard to jurisdictional claims in published maps and institutional affiliations.